

Supporting Information For

HIV-1 Capsid Function is Regulated by Dynamics: Quantitative Atomic-Resolution Insights by Integrating Magic-Angle-Spinning NMR, QM/MM, and MD

Huilan Zhang^{1,2,#}, Guangjin Hou^{1,2,#}, Manman Lu^{1,2}, Jinwoo Ahn^{2,3}, In-Ja L. Byeon^{2,3}, Christopher J. Langmead⁴, Juan R. Perilla⁵, Ivan Hung⁶, Peter L. Gor'kov⁶, Zhehong Gan⁶, William W. Brey⁶, David A. Case⁷, Klaus Schulten⁵, Angela M. Gronenborn^{2,3*}, and Tatyana Polenova^{1,2*}

¹*Department of Chemistry and Biochemistry, University of Delaware, Newark, Delaware 19716, United States;* ²*Pittsburgh Center for HIV Protein Interactions, University of Pittsburgh School of Medicine, 1051 Biomedical Science Tower 3, 3501 Fifth Ave., Pittsburgh, PA 15261, United States;* ³*Department of Structural Biology, University of Pittsburgh School of Medicine, 3501 Fifth Ave., Pittsburgh, PA 15261, United States;* ⁴*Computer Science Department, Carnegie Mellon University, Gates Hillman Center, 5000 Forbes Avenue, Pittsburgh, PA, United States;* ⁵*Department of Physics and Beckman Institute for Advanced Science and Technology University of Illinois at Urbana-Champaign, Urbana, Illinois 61801;* ⁶*National High Magnetic Field Laboratory, Florida State University, Tallahassee, FL, 32310, United States;* ⁷*Department of Chemistry and Chemical Biology, Rutgers University, 174 Frelinghuysen Road, Piscataway, NJ 08854-8087, United States*

#These authors have contributed equally

***Corresponding authors:** Tatyana Polenova, Department of Chemistry and Biochemistry, University of Delaware, Newark, DE, USA, Tel.: (302) 831-1968; Email: tpolenov@udel.edu; Angela M. Gronenborn, Department of Structural Biology, University of Pittsburgh School of Medicine, 3501 Fifth Ave., Pittsburgh, PA 15260, USA, Tel.: (412) 648-9959; Email: amg100@pitt.edu

Classification: Biological Sciences- Biophysics and Computational Biology

Keywords: magic-angle spinning NMR, HIV-1 capsid, CA protein assemblies, HIV-AIDS, conformational dynamics, chemical shift anisotropy, quantum mechanics/molecular mechanics

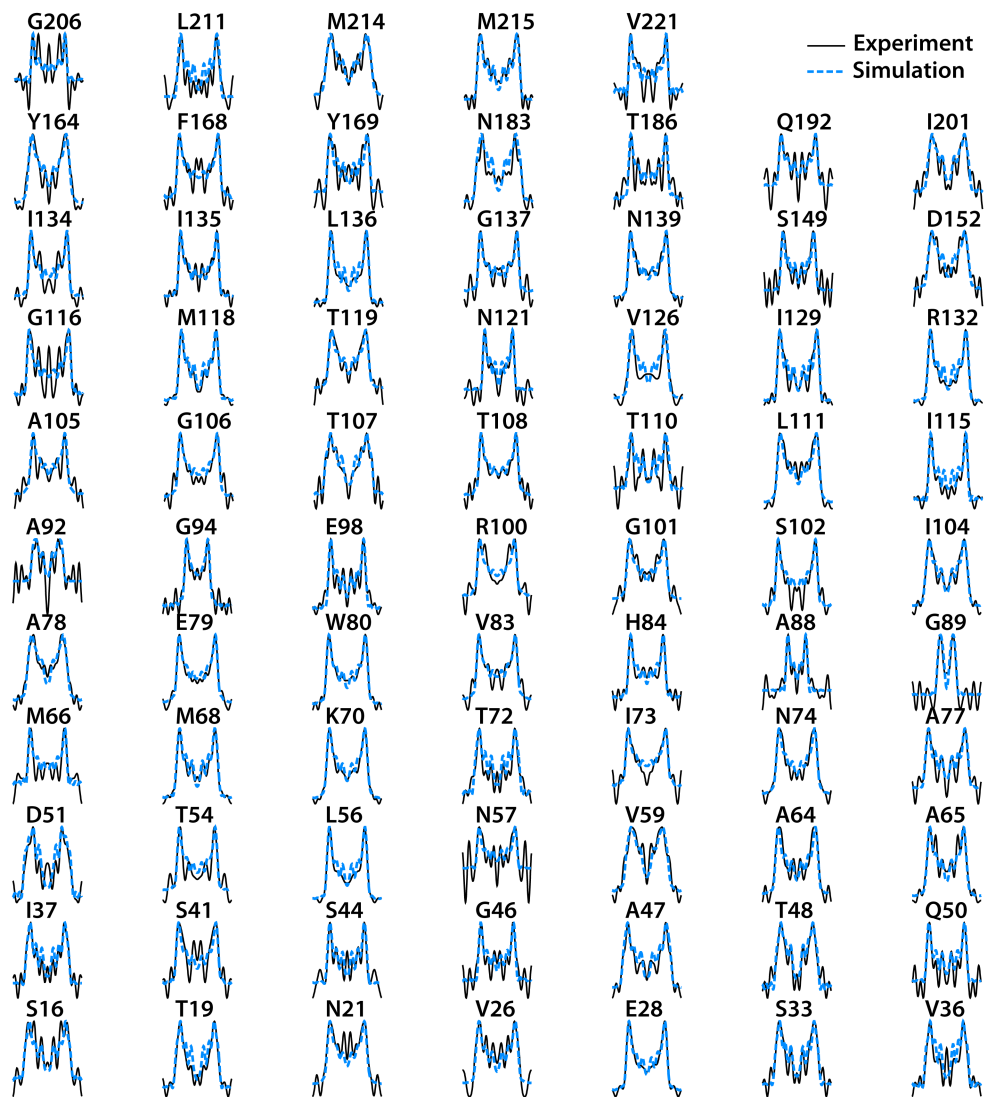


Figure S1. Experimental (solid black lines) and simulated (dashed blue lines) ^{15}N CSA lineshapes for different residues in tubular assemblies of CA HXB2 extracted from the R8_1^3 -RNCSA 3D spectra, recorded at the magnetic field of 21.1 T and the MAS frequency of 14 kHz.

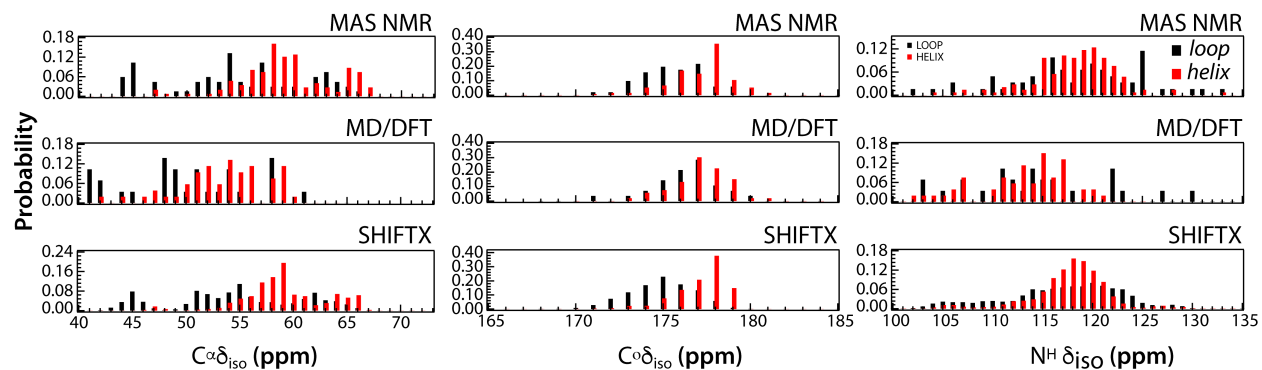


Figure S2. Distribution plots for the isotropic $^{13}\text{C}^\alpha$ (left), $^{13}\text{C}^\circ$ (middle), and $^{15}\text{N}^{\text{H}}$ (right) chemical shifts in HIV-1 CA assemblies. Top: experimental MAS NMR; middle, calculated from MD/DFT; bottom, calculated by SHIFTX as the averaged values over the MD trajectory. The distributions for helical regions are shown in red, for loops- in black.

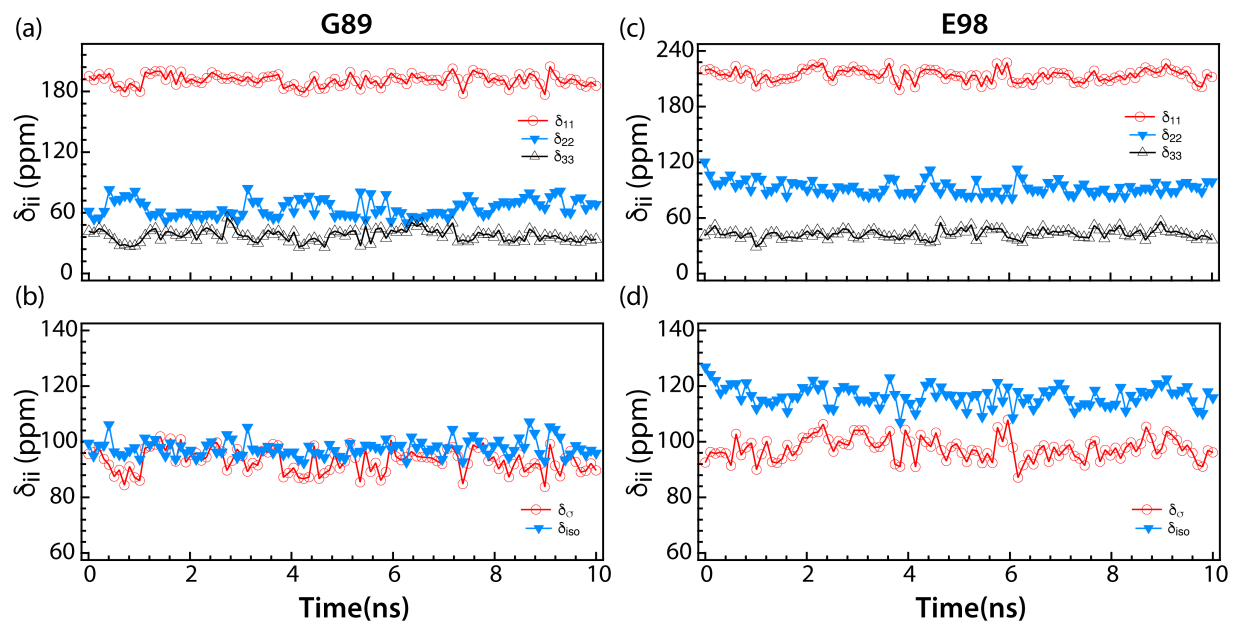


Figure S3. Principal components of ^{15}N CSA tensor, δ_{ii} , δ_{σ} , and δ_{iso} , calculated along the MD trajectory, for selected CA residues: G89 (a, c) and E98 (b, d). For the calculations, 100 frames were used from the first 10 ns of the 100-ns MD trajectory.

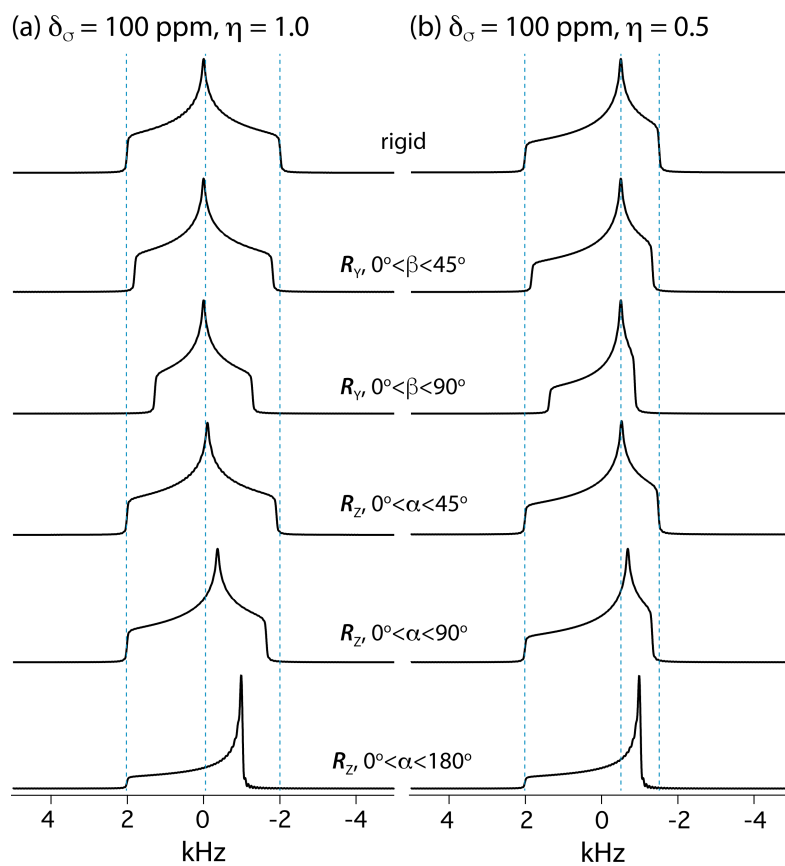


Figure S4. Simulated rigid and motionally reduced ^{15}N CSA line shapes for the sites with the following CSA NMR parameters: (a) $\delta_\sigma = 100$ ppm and $\eta = 1.0$; (b) $\delta_\sigma = 100$ ppm and $\eta = 0.5$. The Euler angles are indicated next to each line shape.

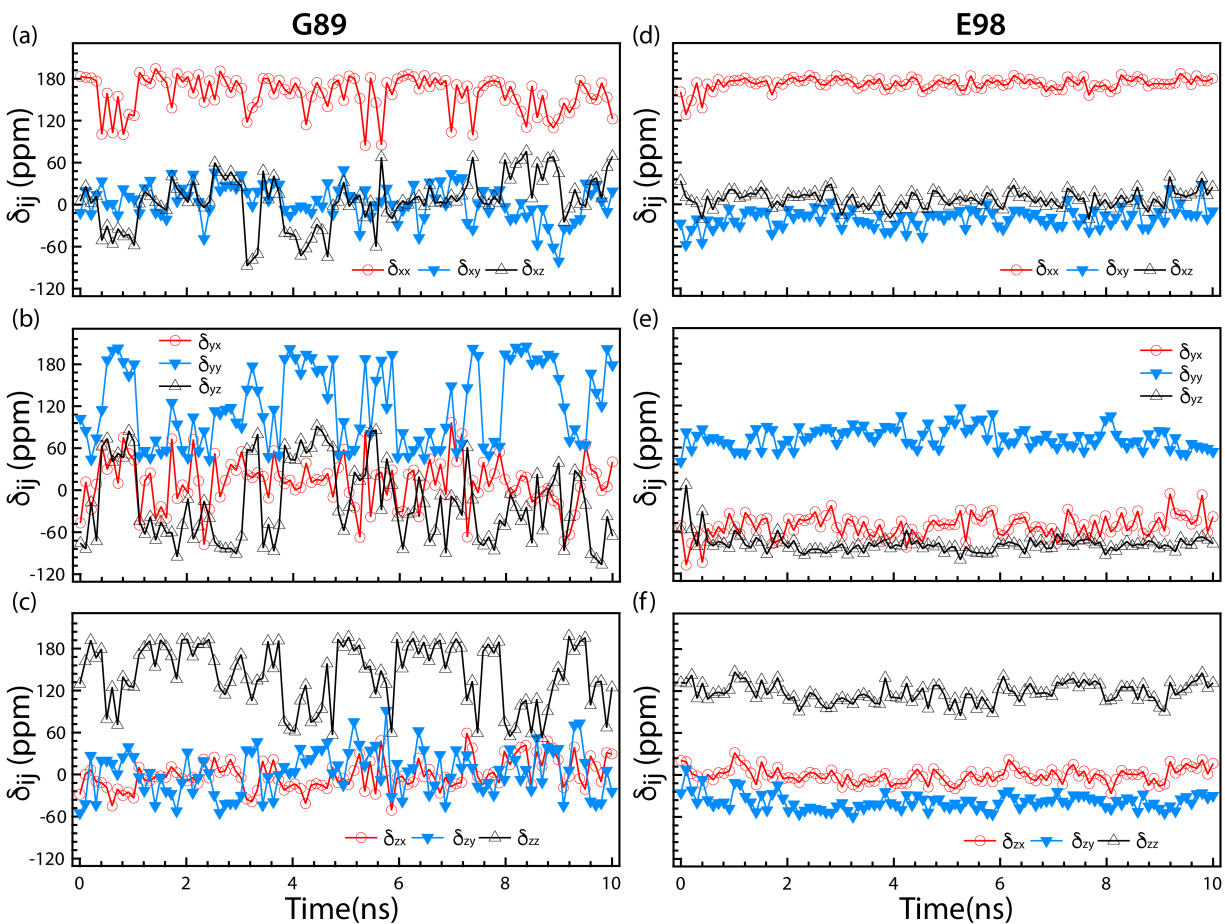


Figure S5. Individual components of ^{15}N CSA tensor δ_{ij} (molecular fixed frame representation), calculated along the MD trajectory, for selected CA residues: G89 (a-c) and E98 (d-f). For the calculations, 100 frames were used from the first 10 ns of the 100-ns MD trajectory.

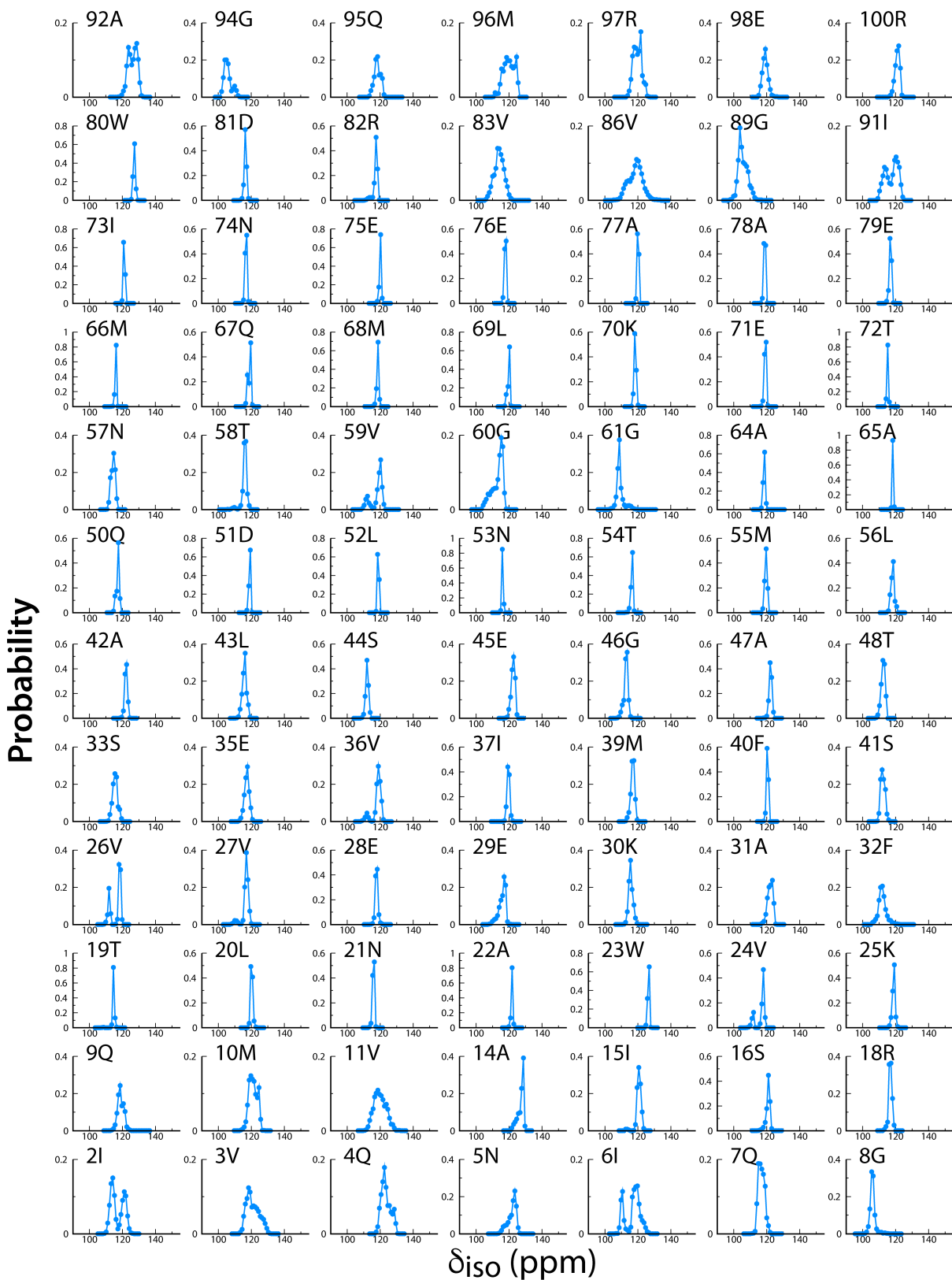


Figure S6. Probability distributions of ^{15}N isotropic chemical shifts of HIV-1 CA calculated by Shiftx based on 5000 frames extracted from 100 ns MD simulation.

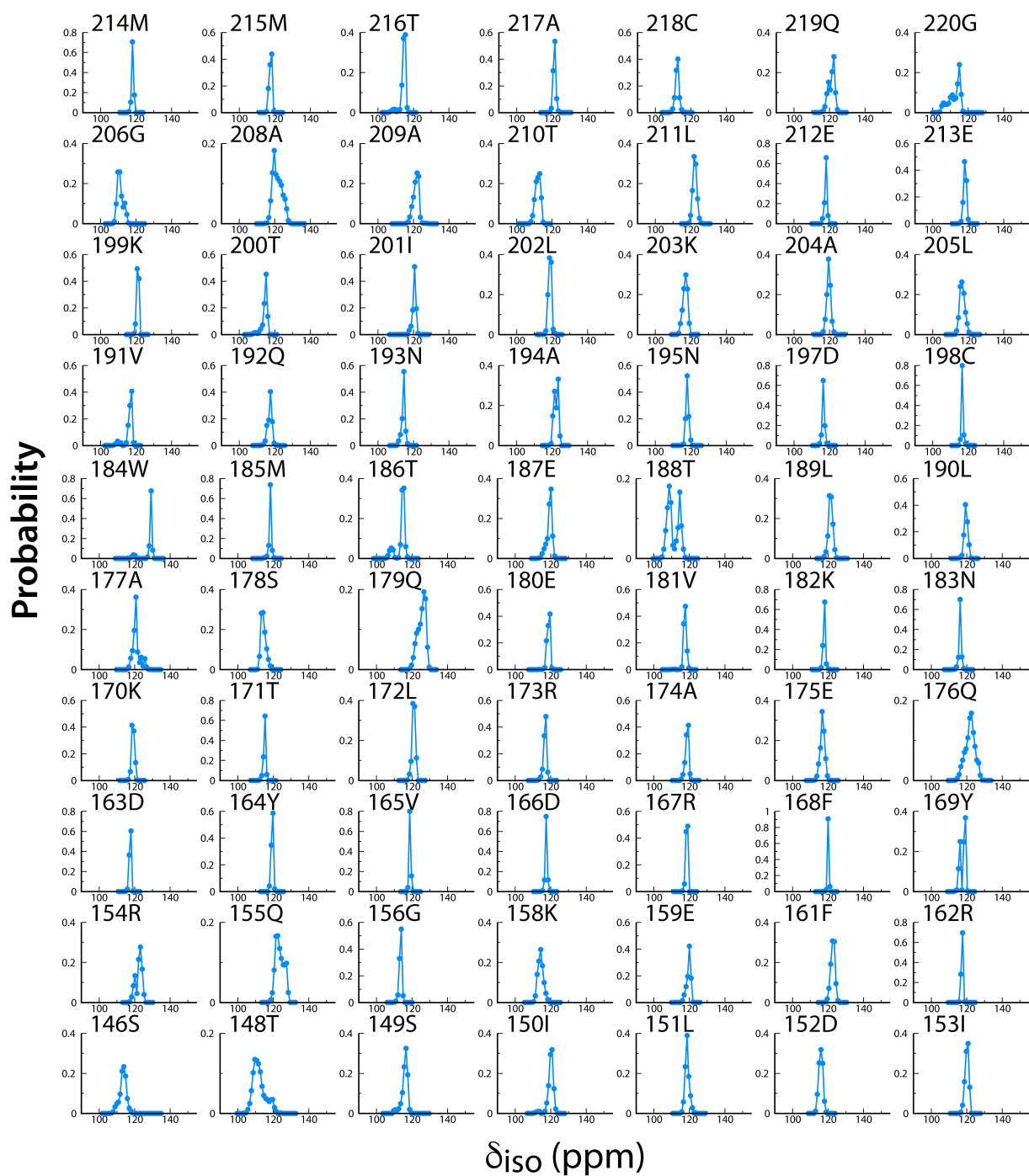


Figure S6. (con'd) Probability distributions of ^{15}N isotropic chemical shifts of HIV-1 CA calculated by Shiftx based on 5000 frames extracted from 100 ns MD simulation.

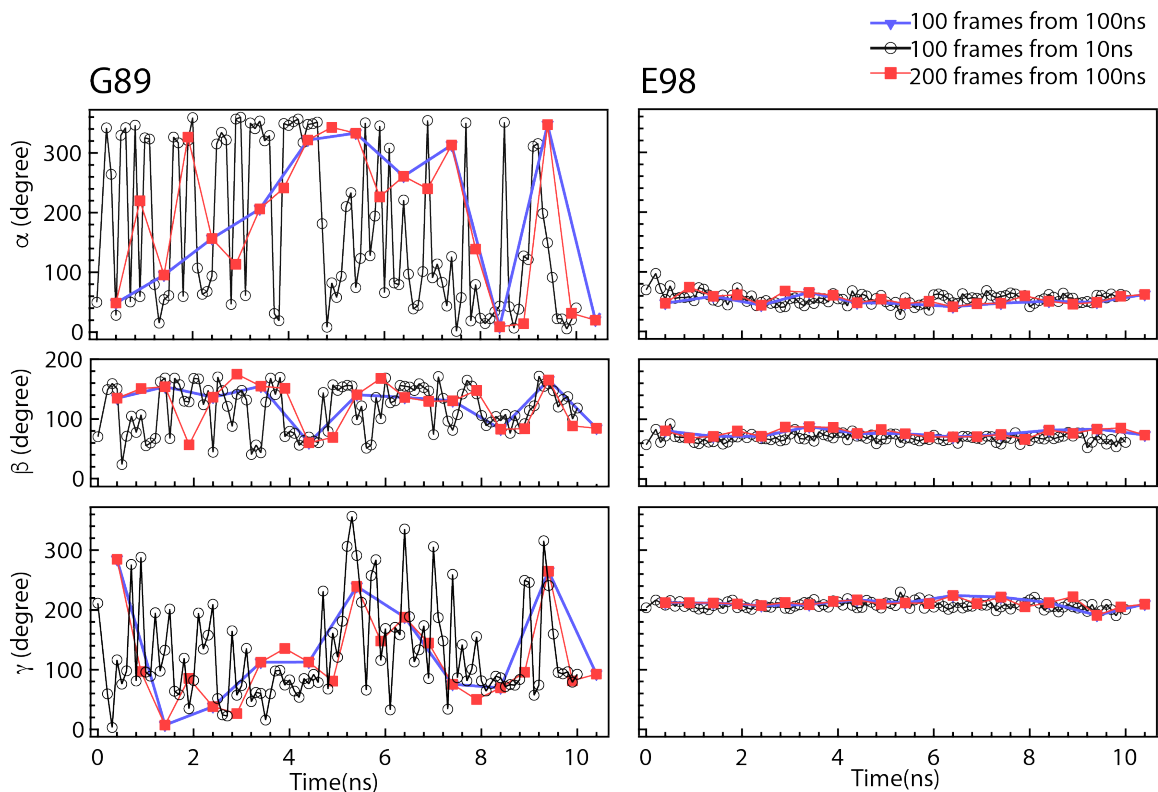


Figure S7. Euler angles of the ^{15}N CSA tensors for G89 and E98 residues of CA, calculated by MD/DFT with different sampling schedules: 200 frames from 100-ns MD trajectory, red; 100 frames from 100-ns MD trajectory, blue; 100 frames from the first 10 ns of the 100-ns MD trajectory, black. The corresponding ^{15}N CSA parameters for G89 are: $\delta_\sigma = 28.92$ ppm, $\eta_\sigma = 0.11$; $\delta_\sigma = 23.28$ ppm, $\eta_\sigma = 0.10$; $\delta_\sigma = 23.75$ ppm, $\eta_\sigma = 0.12$. The corresponding ^{15}N CSA parameters for E98 are: $\delta_\sigma = 93.83$ ppm, $\eta_\sigma = 0.52$; $\delta_\sigma = 93.00$ ppm, $\eta_\sigma = 0.53$; $\delta_\sigma = 92.94$ ppm, $\eta_\sigma = 0.54$.

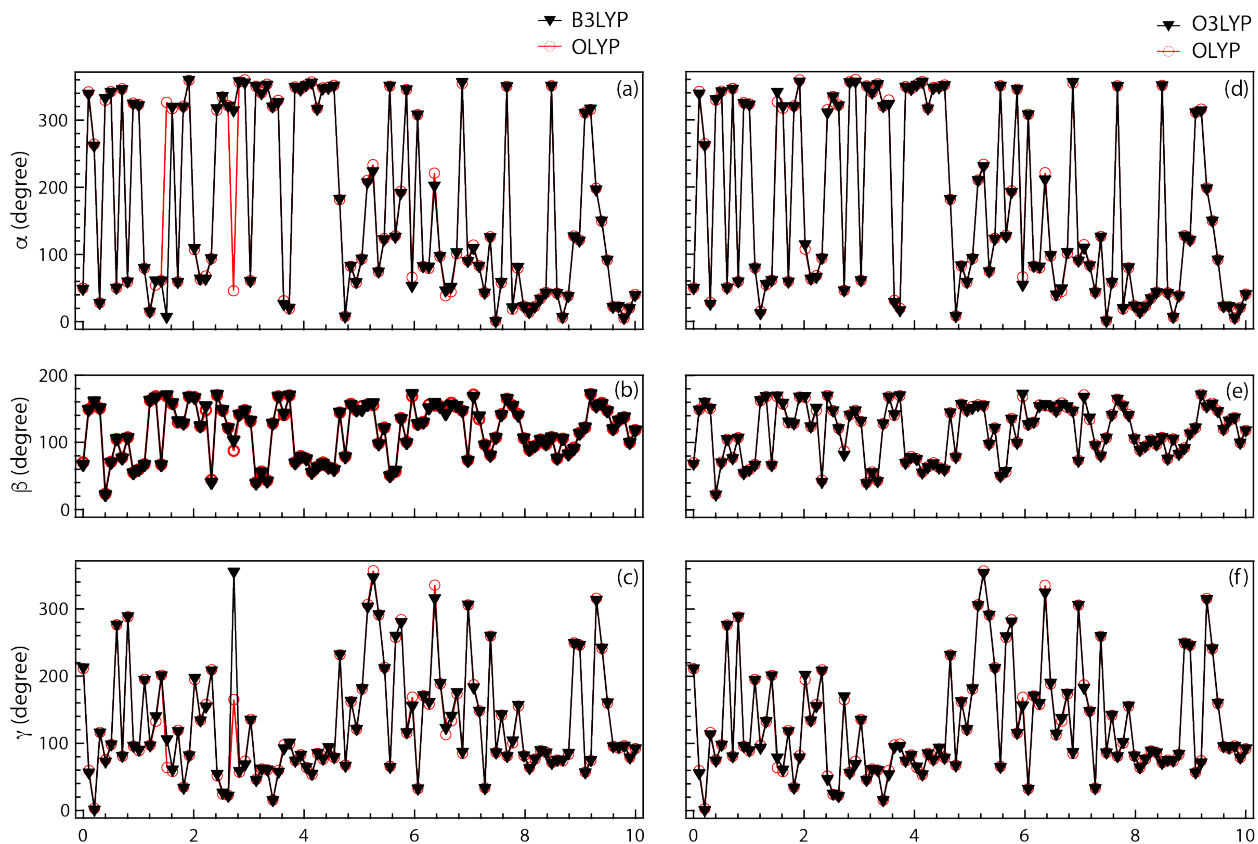


Figure S8. Euler angles of the ^{15}N CSA tensors for G89 residue in the molecular frame along the MD trajectory, calculated using (a-c) B3LYP and OLYP functionals (black and red symbols, respectively), and (d-f) O3LYP and OLYP functionals (black and red symbols, respectively). The angles were calculated using $\delta_{\sigma} = 25.63$, 23.75 , and 24.66 ppm for B3LYP, OLYP, and O3LYP, respectively. Note that the differences are small for δ_{σ} computed with the three functionals. For the calculations, 100 frames were used from the first 10 ns of the 100-ns MD trajectory.